BBA - Molecular Basis of Disease 1863 (2017) 3254–3264

Contents lists available at ScienceDirect

BBA - Molecular Basis of Disease

journal homepage: www.elsevier.com/locate/bbadis

MDA-MB-231 breast cancer cells fuel osteoclast metabolism and activity: A new rationale for the pathogenesis of osteolytic bone metastases

Silvia Lemma[a,b], Gemma Di Pompo[a,b], Paolo E. Porporato[c,1], Martina Sboarina[c], Shonagh Russell[d], Robert J. Gillies[d], Nicola Baldini[a,b], Pierre Sonveaux[c,2], Sofia Avnet[a,*,2]

[a] Orthopaedic Pathophysiology and Regenerative Medicine Unit, Istituto Ortopedico Rizzoli, Bologna, Italy
[b] Department of Biomedical and Neuromotor Sciences, University of Bologna, Bologna, Italy
[c] Pole of Pharmacology, Institute of Experimental and Clinical Research (IREC), Université catholique de Louvain (UCL), Brussels, Belgium
[d] Department of Cancer Imaging and Metabolism, H. Lee Moffitt Cancer Center and Research Institute, Tampa, Florida, United States

ARTICLE INFO

Keywords:
Bone metastases
Osteoclast
Breast cancer
Lactate
Tumor metabolism

ABSTRACT

Recent progress in dissecting the molecular paracrine circuits of cancer and stromal cells in bone metastases (BM) are offering new options to improve current merely palliative approach. The study of tumor-stroma metabolic interplay may further ameliorate this scenario. In this context, we demonstrated that highly glycolytic MDA-MB-231 cancer cells, that form osteolytic BM *in vivo*, release a large amount of lactate at a significantly higher level than MCF7 cells. Thus, we speculated that lactate released from carcinoma cells is uptaken and metabolically used by osteoclasts, the key players of osteolysis associated with BM. First, we demonstrated that the release of lactate at the bone site is mediated by monocarboxylate transporter 4 (MCT4), as revealed by immunostaining and MCT4 localization at the plasma membrane of tumor cells in mouse model of BM and in human tissue sections of BM. Then, we showed that *in vitro* lactate is uptaken by osteoclasts to be used as a fuel for the oxidative metabolism of osteoclasts, ultimately enhancing Type I collagen resorption. The passive transport of lactate into osteoclasts was mediated by MCT1: MCT1 expression is significantly upregulated during osteoclast differentiation and Type I collagen resorption is significantly impaired when osteoclasts are treated with 7-(N-benzyl-*N*-methylamino)-2-oxo-2H-chromene-3-carboxylic acid, an MCT-1 inhibitor. Together, these data demonstrate that lactate released by glycolytic breast carcinoma cells in the bone microenvironment promotes the formation of osteolytic lesions, and provide the rationale for further studies on the use of MCT1 targeting as a novel therapeutic approach in advanced cancer patients with BM.

1. Introduction

Bone is one of the most common sites of solid tumor metastasis, especially for breast carcinomas that cause osteolytic lesions in 80% of patients with stage IV metastatic disease [1]. Osteolytic metastases are characterized by increased osteoclastic activity and bone destruction. To efficiently resorb bone, cancer cells also activate bone cells that are physiologically engaged in bone remodeling, the osteoclasts [2]. Osteoclasts derive from hematopoietic precursors that differentiate into multinucleated cells upon stimulation by receptor activator of NF-κB ligand (RANKL) and macrophage colony-stimulating factor (M-CSF) [3]. Osteolytic bone metastases (BM) are associated with significant morbidity, including hypercalcemia [4], intractable pain, pathological fractures, and spinal cord and nerve root compression [5], ultimately resulting in restricted mobility and a strongly reduced quality of life. Current therapies are mainly palliative and are based on a multidisciplinary approach that includes analgesia, radio/chemotherapy, surgery, hormonal therapy, opioids and bisphosphonates.

Abbreviations: 7ACC2, 7-(N-benzyl-*N*-methylamino)-2-oxo-2H-chromene-3-carboxylic acid; BM, bone metastases; CM, conditioned medium; CTSK, cathepsin K; ECAR, extracellular acidification rate; FCCP, carbonyl cyanide 4-trifluoromethoxy phenylhydrazone; GLUT1, glucose transporter 1; IGF-2, insulin-like growth factor-2; IL-6, interleukin-6; mtOCR, mitochondrial OCR; M-CFS, macrophage colony-stimulating factor; MCT, monocarboxylate transporter; MMP9, matrix metallo proteinase 9; MSC, mesenchymal stromal cells; OCR, oxygen consumption rate; OPG, osteoprotegerin; PBMC, peripheral blood mononuclear cells; RANK, receptor activator of NF-κB; PTHrP, parathyroid hormone-related peptide; RANKL, receptor activator of NF-κB ligand; TBP, TATA-binding protein; TCA, tricarboxylic acid; TGF-β, transforming growth factor β; TNF-α, tumor necrosis factor-α; TRACP, tartrate-resistant acid phosphatase

* Corresponding author at: Orthopaedic Pathophysiology and Regenerative Medicine Unit, Istituto Ortopedico Rizzoli (IOR), via di Barbiano 1/10, 40136 Bologna, Italy.
E-mail address: sofia.avnet@ior.it (S. Avnet).
[1] Present address: Department of Molecular Biotechnology and Health Sciences, University of Turin, Torino, Italy.
[2] Co-last authors.

http://dx.doi.org/10.1016/j.bbadis.2017.08.030
Received 21 March 2017; Received in revised form 23 August 2017; Accepted 28 August 2017
Available online 01 September 2017
0925-4439/

BM develop during the late stages of tumor progression as a result of a multistep process that relies on overcoming multiple barriers to cancer cell dissemination. To successfully metastatize, cancer cells need to enter blood or lymphatic vessels to reach suitable sites, characterized by specific local interactions with the host cells [6]. When cancer cells arrive in bones, cell-cell interactions increase in complexity [7], and the hypoxic conditions of this environment, that are particularly favorable for tumor growth and invasion [8], possibly also play a role. Cancer cells and host cells of bone microenvironment establish an active crosstalk that promotes a vicious circle of tumor growth and bone resorption [9]. Cancer cells secrete factors that stimulate osteoclast-mediated bone resorption, promoting the release of numerous factors from the bone matrix that ultimately drive cancer cells aggressiveness [10]. Among these factors, parathyroid hormone-related peptide (PTHrP) [11] binds to receptors expressed on cells of the osteoblastic lineage that in turn release RANKL and M-CSF and reduce the production of the RANK decoy receptor osteoprotegerin (OPG). RANKL binds its RANK receptor on both osteoclast precursors and mature osteoclasts, promoting osteoclast recruitment and formation as well as bone resorption activity. In addition, other cytokines in the tumor microenvironment stimulate bone resorption, including tumor necrosis factor-α (TNF-α) [12], interleukin-6 (IL-6) [13] and additional growth factors including insulin-like growth factor-2 (IGF-2) [14] and transforming growth factor-β (TGF-β) [15].

Anti-RANKL strategies can reduce tumor-induced osteoclast formation [16]. However, inhibitors of RANK signaling, such as the anti-RANKL antibody denosumab, are only partially effective and display several side effects [17]. In addition to peptide/proteic factors, specific metabolites are also produced by the metabolically altered cancer cells, and these metabolites may be relevant for the pathogenesis of BM. Several oncogenes and tumor suppressor signaling pathways are key regulators of cancer metabolism and modulate the cellular response to alterations of the extracellular microenvironment during tumor progression [18,19]. For example, intratumoral hypoxia causes cancer cells to rely on glycolysis for survival, anabolic growth and proliferation [20]. Notably, proliferating cancer cells often rely on glycolysis also irrespectively of the presence of oxygen (Warburg effect) [21]. Aerobic glycolysis is a hallmark of advanced cancers [22], and is characterized by an increase in glucose uptake, lactate production, and proton release in the tumor microenvironment [23]. Lactate is not a mere waste product of glycolysis, but rather a major player in tumor aggressiveness. Notably, elevated serum lactate in cancer patients is associated with a poor prognosis [24]. Lactate can indeed be captured by oxidative cancer cells, as well as by cells of the tumor-associated stroma, including endothelial cells [25,26] and tumor-associated mesenchymal stromal cells [27] that oxidize it into pyruvate to feed the tricarboxylic acid (TCA) cycle [28].

We have recently demonstrated that osteoclast differentiation is mainly supported by mitochondrial oxidative metabolism which operates in combination with glycolysis to support peripheral cellular activities, including bone matrix degradation, and ensures cell survival during the energy-consuming process of bone destruction [29].

Here, we report that lactate produced by BM-prone glycolytic breast carcinoma cells fuels the oxidative metabolism of osteoclasts, thereby promoting osteolysis.

2. Materials and methods

2.1. Cell culture

Human MDA-MB-231 and MCF7 breast carcinoma cell lines (American Type Culture Collection) were maintained in Iscove's modified Dulbecco's medium (IMDM, Gibco), plus 20 U/mL penicillin, 100 mg/mL streptomycin, and 10% heat-inactivated FBS (complete IMDM), and cultured at 37 °C in a humidified 5% CO_2 atmosphere. Conditioned medium (CM) was collected from MDA-MB-231 cells cultured in DMEM (Sigma) with 25 mM glucose (Merck), 10% heat-inactivated characterized FBS (Celbio), plus 20 U/mL penicillin, 100 mg/mL streptomycin (Euroclone) for 72 h, centrifuged and stored at − 20 °C until use.

2.2. Human osteoclast cultures

Primary cultures of osteoclasts were obtained from monocytic precursors isolated from fresh buffy coats of 35 healthy volunteers (AVIS, Bologna, Italy; Saint-Luc University Clinics, Brussels, Belgium), as previously described [29]. Buffy coats obtained from AVIS were collected after their expiration date (1 day after harvesting), and those from Saint-Luc University Clinics immediately after harvesting. Protocols were approved by Institutional Review Boards. Briefly, peripheral blood mononuclear cells (PBMC) were layered over Hystopaque (GE Healthcare) and seeded (3,000,000 cells/cm^2) in DMEM (Sigma) supplemented with 25 mM glucose (Merck), 10% heat-inactivated characterized FBS (Celbio), plus 20 U/mL penicillin and 100 mg/mL streptomycin (Euroclone), and incubated at 37 °C in a humidified 5% CO_2 atmosphere. All experiments were performed in pyruvate-, lactate-, and glutamine-free medium (complete DMEM), unless stated otherwise.

After 2 h, medium was discarded and replaced with new pro-osteoclastogenic media with a composition depending on the experimental conditions. To evaluate MCT expression and osteoclast metabolism, complete DMEM with glucose (25 mM), RANKL (50 ng/mL) and M-CSF (10 ng/mL) (Peprotech) (pro-osteoclastogenic medium) was used. To evaluate osteoclastogenesis and osteoclast activity in the presence of exogenous or tumor-derived lactate, medium contained 2 mM glucose and either 10 mM of sodium lactate (Sigma) or 25% of CM from MDA-MB-231 cells. Where indicated, MCT1 inhibitor 7-(N-benzyl-*N*-methylamino)-2-oxo-2H-chromene-3-carboxylic acid (7ACC2) was used at 1 μM concentration [30]. 7ACC2 were kindly provided by Olivier Feron (Université Catholique de Louvain). To verify osteoclast differentiation occurring after 5–7 days of culture, cells were analyzed for tartrate-resistant acid phosphatase (TRACP) activity by cytochemistry (Acid phosphatase leukocyte assay, Sigma) and stained with Hoechst 33258 (Sigma). Only TRACP-positive cells with more than three nuclei were considered as osteoclasts.

2.3. qRT-PCR

Total RNA was extracted using the NucleoSpin RNA II (Macherey-Nagel). On-column DNase digestion was performed according to manufacturer's instructions. When RNA was isolated from cells under hypoxic conditions (1% O_2), cells were first plated and incubated for 24 h in a standard incubator, then transferred to a hypoxic incubator (Invivo2-400; Ruskin Technologies) and maintained at 1% O_2 for an additional 24 h. Total RNA (1 μg) was reverse-transcribed into cDNA using MuLV reverse transcriptase and RNase inhibitor (Applied Biosystems) and random hexamers (Applied Biosystems). qRT-PCR was performed by using a Light Cycler instrument and the universal probe library system (Roche Applied Science). Probes and primers are listed in Table 1. PCR protocol was: 95 °C for 10 min; 95 °C for 10 s, 60 °C for 30 s, and 72 °C for 1 s for 45 cycles; 40 °C for 30 s. Expression of genes of interest was normalized using β-actin as a reference gene for MDA-MB-231 and MCF7 cell lines, and TATA-binding protein (TBP) for osteoclasts and precursor cells [31]. Relative expression of candidate genes was calculated using the ΔΔCt model [32].

2.4. SDS-PAGE and immunoblotting

PBMC were seeded on cell culture dishes and maintained in pro-osteoclastogenic media up to 14 days. MDA-MB-231 and MCF7 cells were seeded in 100-mm culture dishes in complete IMDM for 24 h in normoxic (21% O_2) or hypoxic (1% O_2) conditions. Cells were harvested in RIPA buffer [50 mM Tris pH 7.6, 150 mM NaCl, 5% Triton X-

Table 1
Probes and primers.

Gene	Full name	Accession number	Primers	Probe
β-Actin	Actin, beta	NM_001101.2	F = ccaccgcgagaagatga R = ccagaggcgtacagggatag	64
TBP	TATA-binding protein	NM_001172085.1	F = ttgggttttccagctaagttct R = ccaggaaataactctggctca	24
MCT1/SLC16A1	Monocarboxylate transporter 1	NM_003051.3	F = ggattggtgaccattgtgg R = catgtcattgagccgaccta	56
MCT4/SLC16A3	Monocarboxylate transporter 4	NM_001206952	F = gagtttgggatcggctacag R = cggttcacgcacacactg	58
GLUT1	Glucose transporter 1	NM_006516.2	F = ggttgtgccatactcatgacc R = cagataggacatccagggtagc	67
MMP9	Matrix metallopeptidase 9	NM_004994.2	F = gaaccaatctcaccgacagg R = gccacccgagtgtaaccata	6
CTSK	Cathepsin K	NM_000396.3	F = ggatatgttactcctgtcaaaaatca R = tgccagttttcttcttgagttg	37

100, 0.25% sodium deoxycholate, 1 mM EGTA pH 8, 1 mM NaF] (Sigma) containing protease and phosphatase inhibitor cocktails (Roche). Protein lysates were quantified by using the BCA protein assay (Pierce), subjected to reducing SDS-PAGE on polyacrylamide gels and transferred onto nitrocellulose membranes (Thermo Fisher Scientific). Membranes were stained with Ponceau red (Sigma) to confirm equal protein loading. Blots were probed with anti-MCT1 (Chemicon, AB3538P), MCT4 (Santa Cruz, sc-50329), and β-actin (Cell Signaling, 4970s) primary antibodies, followed by horseradish peroxidase-conjugated secondary anti-mouse and anti-rabbit antibodies (GE Healthcare), as appropriate. To detect different proteins on the same blot, nitrocellulose membranes were stripped with Restore Western blot stripping buffer (Thermo Fisher Scientific) and reprobed. Proteins were visualized with a chemiluminescence substrate (ECL Western blotting detection reagent, GE Healthcare). The signal of each band was quantified by the VisionWorksLS analysis software (Biospectrum, UVP) for densitometric evaluation. Results are representative of four biological replicates.

2.5. Immunostaining analysis

Procedures involving animals and their care were conducted with national committee approval (licence number ESAVI-2077-04) and conformed to national and international laws and policies (EEC Council Directive 86/609, OJ L 358, 1, Dec. 12, 1987; NIH guide for the Care and Use of Laboratory Animals, NIH Publication No. 85–23, 1985). Five-six-week-old female athymic nude mice (Foxn1^{nu}, Envico, Netherlands) were anaesthetized with analgesic (Temgesic; buprenorphine 0,1 mg/kg, s.c.), and injected with MDA-MB-231 cells into the bone marrow of right proximal tibia (1×10^5 cells/20 μL PBS). Mice were sacrified 29 days after inoculation of cancer cells. Paraffin-embedded tumor-bearing tibias were de-calcified in EDTA and dehydrated. 4 μm sections were obtained and deparaffined and rehydrated for immunostaining. TRACP-staining sections were obtained by using Pararosaniline (Sigma-Aldrich). TRACP was used as a specific marker of osteoclasts. The sections were incubated in 3% perhydrol solution to block the endogenous peroxidase reaction. Nonspecific binding was blocked by incubation in 5% bovine serum albumin. The following primary antibodies were used: rabbit Ab anti-MCT1 (HPA003324, Sigma) and rabbit anti-MCT4 (sc-50,329, Santa Cruz). Sections were washed, incubated with a biotinylated secondary antibody, covered with DAB and counterstained with Mayer's hematoxylin. Negative controls were also performed by omitting the primary antibody.

Experiments using human tumor biopsies were approved by the local Ethical Committee (approval No 0037602 of 14 November 2013) and performed with the informed consent of the patient. Human BM samples were obtained during the surgical excision of the tumor mass of 4 patients with breast carcinoma, and immediately frozen. Biopsies were embedded in Optimal Cutting Temperature compound (Miles Laboratories), and frozen on dry ice before sectioning. Immunofluorescence assays were performed on the tumor sections and on PBMC cultured on glass coverslips with pro-osteoclastogenic medium until osteoclasts formed. Sections with a thickness of 7 μm were mounted on glass slides covered with 2% saline solution in acetone, and stored at − 20 °C. Osteoclasts were fixed in 4% paraformaldehyde. Defrosted sections and osteoclasts were permeabilized with 0.2% Triton X-100, blocked with 1% BSA, and then incubated with primary rabbit anti-MCT4 (sc-50329, Santa Cruz), and mouse anti-cytokeratin (M0821, Dako) antibodies. As secondary antibodies, we used anti-rabbit Alexa Fluor 488 nm (A1108, Life Technologies), anti-rabbit Alexa Fluor 568 nm (A11011, Life Technologies) and anti-mouse Alexa Fluor 488 (A10680, Life Technologies). Nuclei were stained with Hoechst 33258 (Sigma). Images were acquired by using confocal microscopy Nikon TI-E.

2.6. Oxygen consumption and extracellular acidification

Oxygen consumption rate (OCR) and extracellular acidification rate (ECAR) were determined using a Seahorse XF96 extracellular flux analyzer and a Mito Stress kit (Seahorse Biosciences). PBMC were seeded on XF96 microplates in pro-osteoclastogenic medium until osteoclasts formed. Then, the medium was replaced by fresh complete medium with/without 10 mM of sodium lactate. Cells were analyzed 7 days later. MDA-MB-231 and MCF7 cells were seeded on XF96 microplates in complete IMDM for 24 h. Culture media were replaced by base medium (non-buffered DMEM supplemented with 25 mM glucose) 1 h before analysis. Selective inhibitors were injected during measurements: oligomycin (2 μM), carbonyl cyanide 4-trifluoromethoxy phenylhydrazone (FCCP; 0.9 μM), rotenone (1 μM), antimycin A (1 μM) and 2-deoxy-glucose (100 mM). Mitochondrial OCR (mtOCR) was calculated by subtracting non-mitochondrial OCR (the level obtained after injection of rotenone and antimycin A) from total OCR levels. ATP coupling was calculated by subtracting total OCR from oligomycin readings. Data were normalized for total protein content using the Bradford protein assay (Bio-Rad).

2.7. NADH/NAD$^+$ analysis

NAD$^+$ and NADH levels were measured using a NAD$^+$/NADH quantitation kit (Sigma). Briefly, 2×10^5 MDA-MB-231 or MCF7 cells were lysed according to manufacturer's instructions. NAD$^+$ levels were measured by subtracting NADH concentration from total NAD concentration. Data were normalized to total protein content determined using the BCA protein assay.

2.8. Lactate and glucose measurements

For enzymatic lactate determination, 2.6×10^4 MCF7/cm^2 and 4.0×10^4 MDA-MB-231/cm^2 were plated into 12-well plates in complete IMDM. After 24 h, medium was replaced by DMEM (Sigma) supplemented with 20 mM glucose (Merck), 10% FBS (Euroclone) plus 4 mM L-glutamine, 20 U/mL penicillin, and 100 mg/mL streptomycin (complete DMEM for carcinoma), then maintained in normoxia (21% O_2) or transferred to a hypoxic incubator (Invivo2-400; Ruskin Technologies) and maintained at 1% O_2. Medium was harvested 72 h later to measure the L-lactate concentration using a EnzyChrom L-lactate assay kit (BioAssay Systems). Normalization was performed to total protein content measured by BCA protein assay.

Lactate and glucose concentration were also measured over the time. MDA-MB-231 and MCF7 were seeded on 12-well plates in complete IMDM. After 24 h, medium was replaced by complete DMEM for carcinoma. Supernatant fractions were collected 24–48–72 h later. Metabolite concentrations were quantified using the Lactate-Glo™ Assay and Glucose-Glo™ Assay (Promega), according to manufacturer's instructions. Glucose consumption and lactate production were normalized to the total protein content that was measured by BCA protein assay.

Lactate and glucose consumption were also measured enzymatically in osteoclast culture by analyzing deproteinized cell culture supernatants. PBMCs were seeded on 96-well plates in pro-osteoclastogenic medium and cultured until multinucleated TRACP$^+$ cells were formed. Media were replaced by fresh complete medium with or without sodium lactate (10 mM). Supernatant fractions were collected 7 days later. Metabolite concentrations were quantified using specific enzymatic assays on CMA600 analyzer (CMA Microdialysis AB). Glucose consumption and lactate production were normalized to total protein content measured by a Bradford protein assay.

For ^{14}C-lactate uptake assays, PBMC were seeded on 24-well plates and maintained in pro-osteoclastogenic medium until osteoclast differentiation was confirmed. When multinucleated TRACP$^+$ cells were formed, culture medium was replaced by pro-osteoclastogenic medium containing sodium lactate (10 mM) and cells were incubated overnight for metabolic adaptation. Cells were then rinsed with a modified Krebs solution containing sodium lactate (10 mM) without glucose, and exposed to increasing concentrations of ^{14}C-L-Lactate (1, 2, 4, 8, and 16 μM) or control Krebs solution at 37 °C for 12 min. Cells were rinsed with ice-cold D-lactate-containing Krebs solution and lysed with 0.1 M NaOH. Sample aliquots were then incubated in liquid scintillation solution (Microscint 40) into 96-well plates (Optiplate). After 1 h of stirring, radioactivity was measured on a PerkinElmer Topcount. Cpm values are normalized for protein content measured with a Bradford protein assay.

2.9. Mitochondrial potential measurement

The mitochondrial potential of mature osteoclasts was measured using the cationic dye 5,5′,6,6′-tetrachloro-1,1′,3,3′-tetraethylbenzimidazolylcarbocyanine iodide (JC-1), which exhibits potential-dependent accumulation in mitochondria as revealed by a fluorescence emission shift from green (540 nm) to red (590 nm). PBMCs were cultured in pro-osteoclastogenic medium until osteoclasts formed. Then, medium was replaced by fresh, complete medium with or without sodium lactate (10 mM). Cells were analyzed 7 days later. Cells were incubated with JC-1 (10 μg/mL) for 10 min at 37 °C, then washed with PBS, and analyzed in complete cell culture medium. Analysis was performed using a TiE spectral confocal laser microscope (A1R, Nikon).

2.10. Bone resorption assay

The bone resorption activity of osteoclasts was measured by using the OsteoLyse kit (Lonza). PBMC were cultured in pro-osteoclastogenic medium with or without sodium lactate (10 mM) and with or without MCT1 inhibitor 7ACC2 (1 μM). How these compounds affect the osteoclast behaviour once incubated with MDA-MB-231 cell supernatants was evaluated by culturing PBMC in complete DMEM containing glucose (2 mM) and 25% of CM from MDA-MB-231 cells, with or without 7ACC2 (1 μM) [30]. Cells were cultured until osteoclasts formed. Then, media were renewed for 72 h. Supernatant fractions were collected after 10 days, and the amount of Type I collagen was quantified by the emission of Europium-labelled collagen fragments *via* time-resolved fluorescence (Infinite 200 PRO, Tecan).

2.11. Statistical analysis

Statistical analyses were performed using GraphPad Prism version 5.00 for Windows (GraphPad Software, San Diego California USA, www.graphpad.com). Due to the low number of observations, data were considered not to be normally distributed, and nonparametric statistical tests were used. Specifically, the Mann-Whitney *U* test was used for differences between two groups, the Spearman Rank test was used for the analysis of correlation between two different parameters, and the Pearson's test was used for co-localization analysis. Results were reported as mean ± standard error of mean (SE). *N* indicates the number of independent experiments and *n* the total number replicates per treatment condition. For all the analyses, only $p \leq 0.05$ were considered significant.

3. Results

3.1. Glycolysis and lactate release are increased in the metastatic breast carcinoma cell line MDA-MB-231

As models of breast carcinoma cells with different metastatic potentials, we used human metastatic MDA-MB-231 cells that express high levels of monocarboxylate transporter 4 (MCT4) [33], and MCF7 cells that are not able to form bone metastases in preclinical *in vivo* model when intracardially injected [34]. To study metabolic regulation of BM, we first determined the extracellular acidification rate (ECAR) as a measure of glycolysis and the oxygen consumption rate (OCR) as a measure of oxidative phosphorylation of breast carcinoma cells. We found that metastasis-prone MDA-MB-231 cells have higher ECAR and lower OCR than MCF7 cells (Fig. 1A) and, in more detail, a higher glucose-dependent glycolysis (Fig. 1B, $p < 0.0001$). Consistent with these data, MDA-MB-231 also had a higher NADH/NAD$^+$ ratio than MCF7 cells (Fig. 1C, $p = 0.0476$). Moreover, MDA-MB-231 displayed higher mRNA expression of the glucose transporter GLUT1 than MCF7 cells (Fig. 1D, $p = 0.0143$). GLUT1 expression increased under hypoxic conditions for both cell lines (Fig. 1D, $p = 0.0143$). MDA-MB-231 cells released in the supernatant significantly higher levels of lactate than MCF7 cells in all the evaluated time points (24–48–72 h). These levels reached the concentrations of about 10 mM (Fig. 1E). At the same time points, MDA-MB-231 cells consumed significantly more glucose than MCF7 cells (Fig. 1E). Notably, hypoxic conditions increased the release of lactate in both MDA-MB-231 and MCF7 cells (Fig. 1F, $p = 0.0495$). These results indicate that metastatic MDA-MB-231 cells have high glycolytic metabolism and abundantly release lactate to the extracellular microenvironment, especially in hypoxic conditions, whereas MCF7 cells are more oxidative.

To complete the characterization of the metabolic phenotype of MDA-MB-231 cells, we measured the expression of MCT4, a lactate transporter adapted for lactate release to the extracellular space [35]. We found high levels of MCT4 mRNA and protein expression in MDA-MB-231 cells, whereas MCT1, which usually conveys lactate uptake [36], was almost undetectable (Fig. 1G and H). Comparatively, MCF7 cells expressed significantly lower levels of MTC4 mRNA than MDA-MB-231 cells (Fig. 1G, $p = 0.0035$) and significantly higher levels of MCT1 mRNA, both under normoxia ($p = 0.0022$) and hypoxia

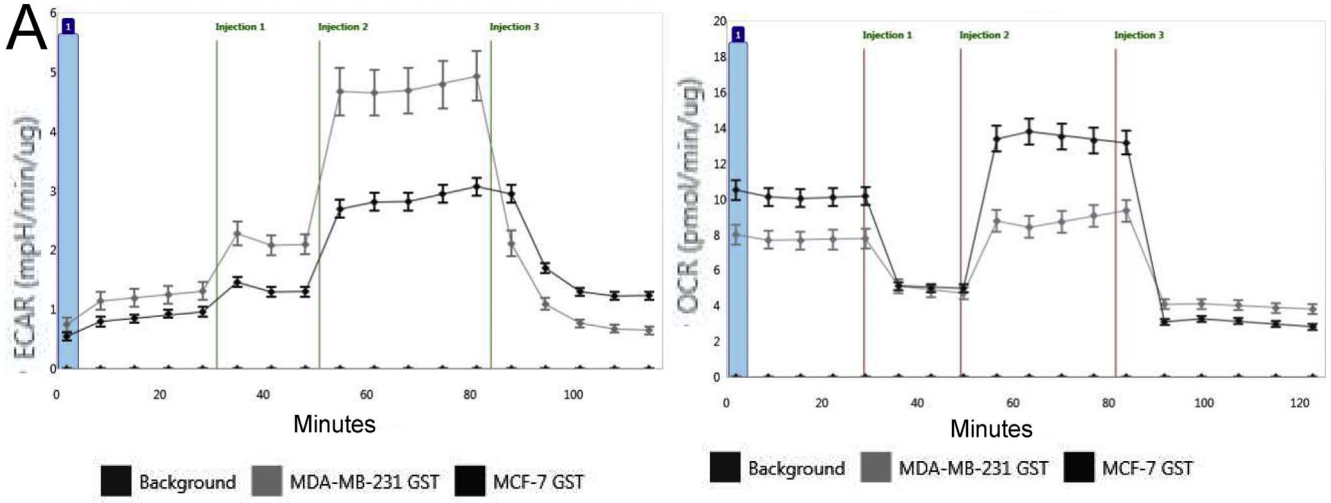

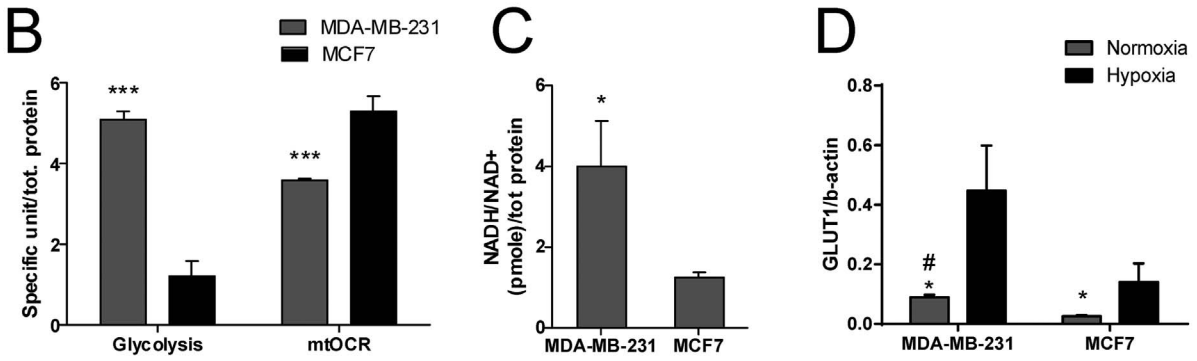

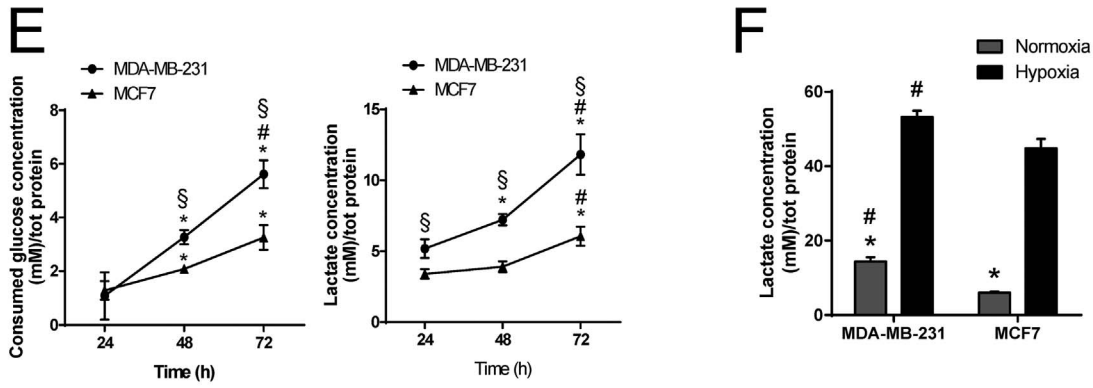

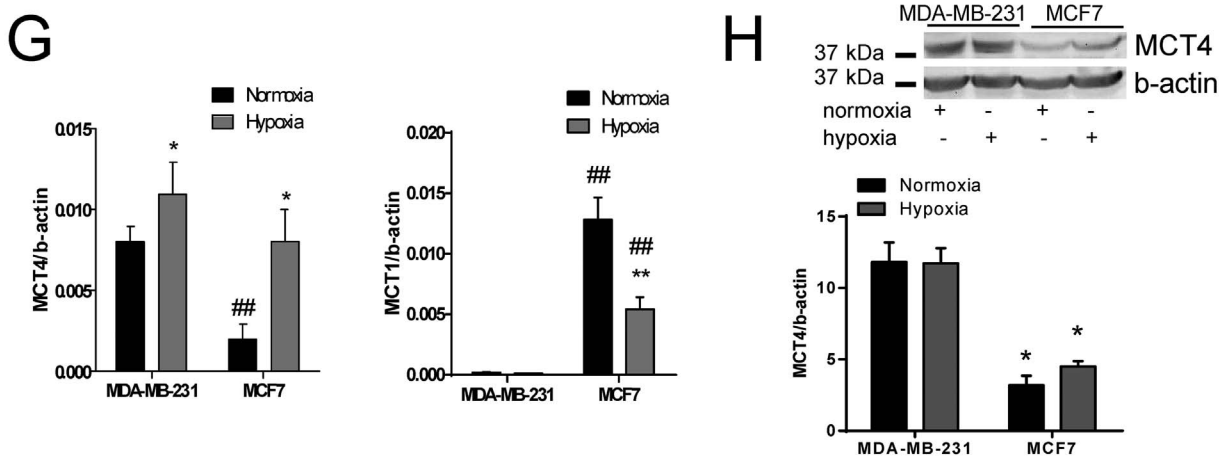

(caption on next page)

Fig. 1. Energetic metabolism in breast carcinoma cells with different aggressiveness. BM-prone MDA-MB-231 cells were metabolically compared with MCF7 cells that are not able to form BM. (a) Representative graphs showing extracellular acidification rate (for ECAR: 1, 2, 3 are the time-points for the injection of glucose, oligomycin and 2-deoxy-D-glucose, respectively) and oxygen consumption rate (for OCR: 1, 2, 3 are the time-points for the injection of oligomycin, FCCP, antimycin A and rotenone, respectively). (b) Glycolysis and mitochondrial OCR (mtOCR). Mean ± SE, $N = 3$, $n = 7$. $^{***}p < 0.0001$ *vs* MCF7. (c) NADH/NAD^+ ratio. Mean ± SE, $n = 5$, $^{*}p < 0.05$ *vs* MCF7. (d) GLUT1 mRNA expression under normoxia and hypoxia (1% O_2). Mean ± SE, $N = 2$, $n = 2$ $\#p < 0.05$ *vs* MCF7; $^{*}p < 0.05$ *vs* hypoxia. (e) Glucose consumed and lactate released in cell supernatants over time. Mean ± SE, $N = 3$, $n = 2$, $^{*}p < 0.05$ *vs* 24 h, $\#p < 0.05$ *vs* 48 h, §$p < 0.05$ *vs* MCF7. The experiment was repeated 3 times with similar results. (f) Lactate released in MDA-MB-231 and MCF7 cell supernatant under normoxia and hypoxia (1%). Mean ± SE, $N = 3$, $n = 2$. $^{*}p < 0.05$ *vs.* hypoxia, $\#p < 0.05$ *vs* MCF7. (g) MCT4 and MCT1 mRNA expression under normoxic and hypoxic (1%) conditions. Mean ± SE, $N = 3$, $n = 2$. $^{*}p < 0.05$ *vs* hypoxia, $\#\#p < 0.01$ *vs* MDA-MB-213. (h) Western blot analysis of MCT4 expression under normoxia and hypoxia (1%). Lower panel, densitometric quantification. Upper panel, representative image. Mean ± SE, $N = 4$, $^{*}p < 0.05$ *vs* MDA-MB-231, p = ns *vs* hypoxia.

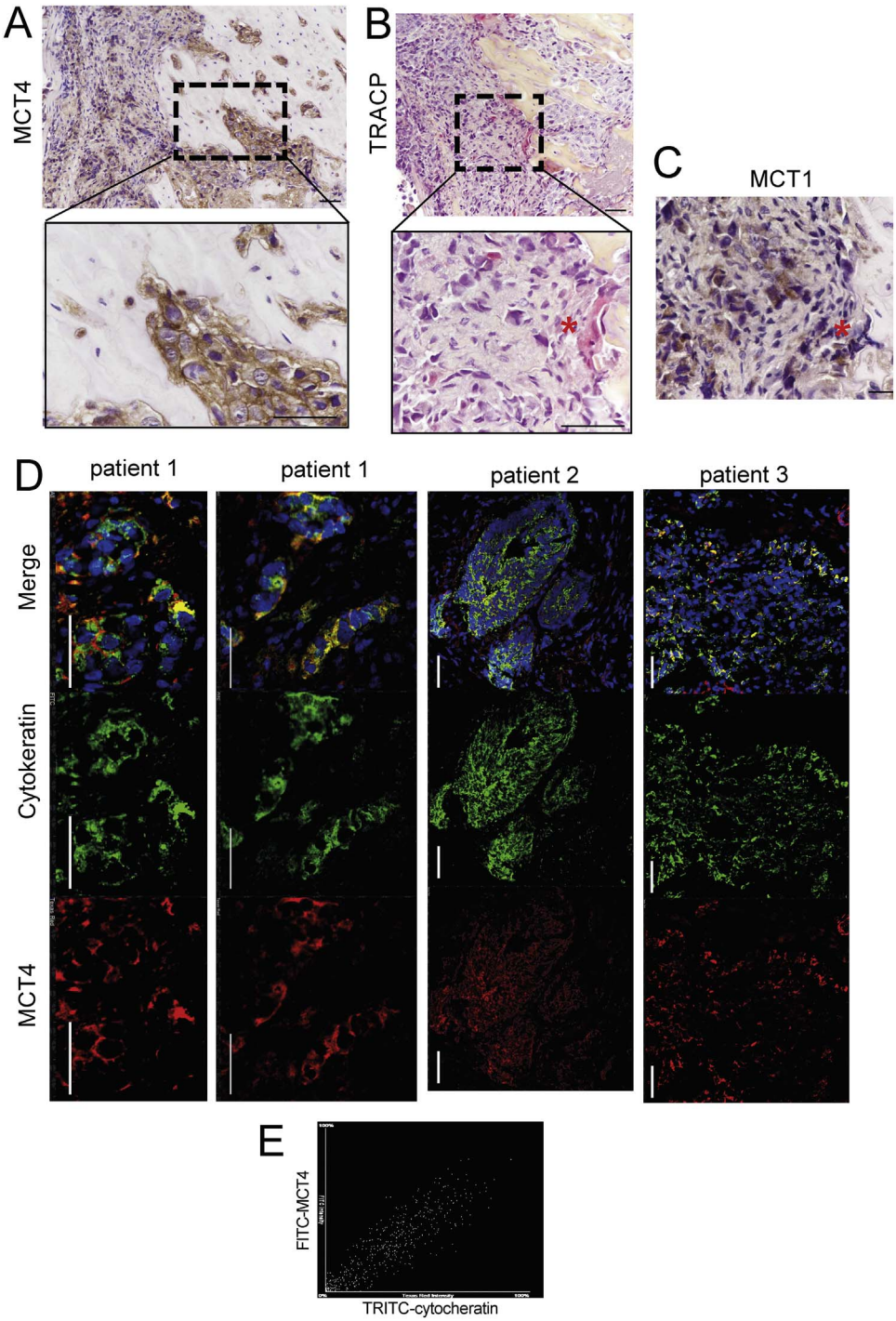

Fig. 2. MCT4 is expressed at the plasma membrane of carcinoma cells in mouse model of BM and in BM clinical samples. (a) Immunostaining of MCT4 in osteolytic bone metastases obtained by the injection in the tibia of human breast carcinoma cells (MDA-MB-231). Scale bar 50 μm. (b) TRACP staining of the same tissue obtained from BM mouse model. The red mark shows a positive multinucleated osteoclast. Scale bar 50 μm. (c) Immunostaining of MCT1 in consecutive tissue section showed in panel b. Red mark shows the same area marked in panel b. Scale bar 50 μm. (d) Representative fields of immunofluorescence staining of MCT4 and confocal analysis of BM sections from different patients with a previous diagnosis of breast cancer. Specific antibodies against cytokeratin (green) and MCT4 (red) were used. Nuclei were counterstained with Hoechst 33258 (blue). Scale bar 50 μm. (e) Image of the analysis of co-localization of MCT4 and Cytokeratin immunostaining by Pearson's correlation test performed in a representative cell of the tissue section showed in panel d.

($p = 0.0040$). Hypoxia significantly increased the mRNA expression of MCT4 in MDA-MB-231 (Fig. 1G, $p = 0.0138$) and in MCF7 cells ($p = 0.0145$), and significantly reduced MCT1 mRNA expression in MCF7 cells (Fig. 1G, $p = 0.0079$). At a protein level, Western blot analysis revealed that MDA-MB-231 expressed higher levels of MCT4 both under normoxia (Fig. 1H, $p = 0.0147$) and hypoxia (Fig. 1H, $p = 0.0143$) with respect to MCF7. Finally, we analyzed the localization of MCT4 and MCT1 in a mouse model of osteolytic metastasis obtained by intratibially injection of human breast carcinoma cells and in BM tissue sample from patients with breast carcinoma. We found a strong staining for MCT4 in tumor cells (Fig. 2A) and a signal for MCT1 in the osteolytic area where osteoclasts are located (red marks in Fig. 2C, osteoclasts are made clear by TRACP staining in a consecutive tissue section in Fig. 2B). For samples from human patients, we used cytokeratin to distinguish cancer cells from the surrounding stroma. MCT4 staining strongly overlapped with cytokeratin staining (Fig. 2D, yellow color in the merged images), as revealed by a significant co-localization (Fig. 2E, the Pearson's test for four different cells in different field corresponded to 0.939, 0.896, 0.850, 0.908), suggesting that aggressive breast cancer cells also abundantly express MCT4 at the bone metastatic site.

3.2. Exogenous lactate fuels the oxidative metabolism of mature osteoclasts

To investigate the ability of human osteoclasts to convey tumor-derived lactate into energetic fuelling, we used sodium L-lactate at 10 mM concentration, within the range of concentration frequently measured in breast carcinoma tumors *in vivo* [37]. This concentration is also the amount released by MDA-MB-231 cells *in vitro* after 72 h of incubation (Fig. 1E). Osteoclasts took up exogenous ^{14}C- lactate (Fig. 3A, $p < 0.0001$), and, when treated with lactate, showed significantly higher ECAR, and even higher mtOCR and ATP coupling efficiency. The increase for mtOCR and ATP coupling efficiency was almost double in respect to not treated cells (Fig. 3B, $p = 0.0465$ for ECAR; $p = 0.001$ for mtOCR and ATP coupling).

The mitochondrial transmembrane potential ($\Delta\psi$) assessed by the fluorescent probe JC-1, and the glycolytic efficiency (lactate production/glucose consumption) [29] confirmed the data obtained with the Seahorse analysis. In fact, lactate uptake significantly increased the $\Delta\psi$ of mature osteoclasts (Fig. 3C, $p = 0.0003$), and promoted a significantly lower glycolytic efficiency (Fig. 3D, $p < 0.0001$). We excluded from the calculation the amount of lactate normally produced by osteoclast in lactate free condition (1 mM/h). These data suggest that exogenous lactate transported into mature human osteoclasts is an oxidative fuel for these cells.

3.3. MCT1 expression increases during osteoclastogenesis

MCT1 is ubiquitously expressed in cells that consume lactate. Thus, we evaluated if this assumption stands in osteoclasts. We analyzed the expression of MCT1 and MCT4 in precursor cells (day 0 at seeding) and mature osteoclasts (at day 7 and after, from seeding). MCT1 mRNA expression increased during osteoclast differentiation, whereas MCT4 mRNA expression was not affected (Fig. 4A). Similarly, MCT1 protein

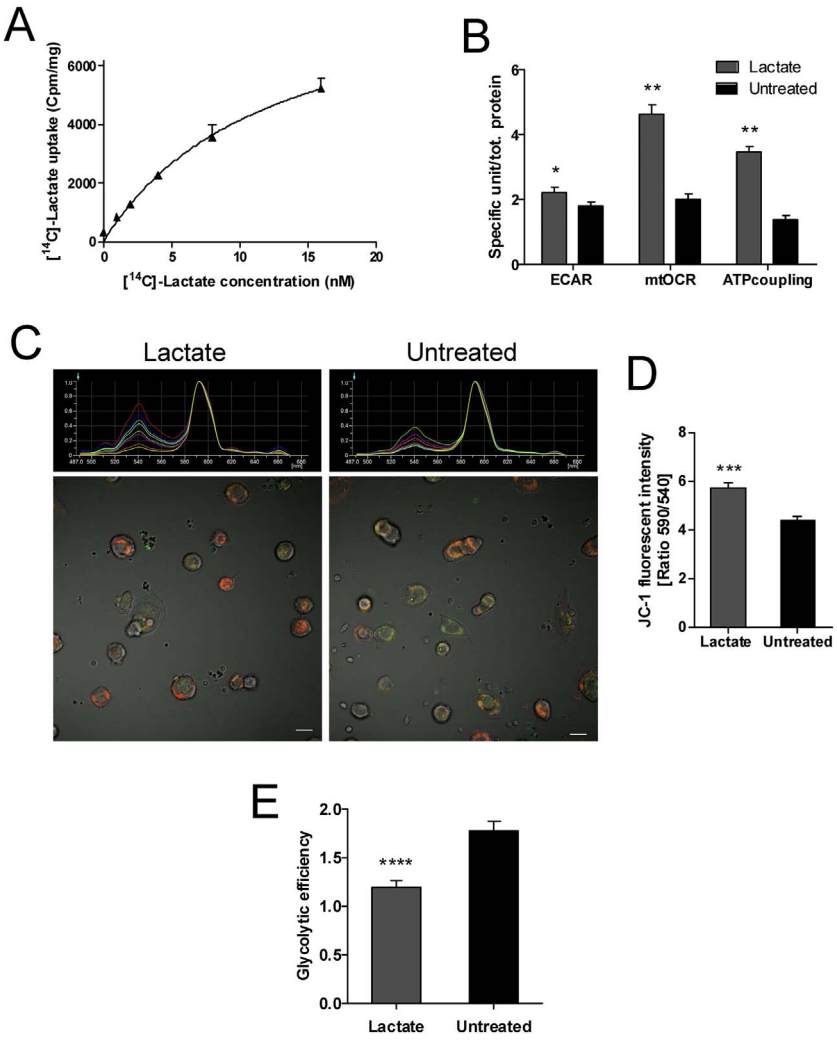

Fig. 3. Lactate fuels the oxidative metabolism of mature osteoclasts. (a) Radiolabeled lactate influx determined by measuring the amount of ^{14}C-lactate that was captured by mature osteoclasts. Mean ± SE, $n = 6$. The experiment was repeated 3 times with similar results. (b) Extracellular acidification rate (ECAR), mitochondrial oxygen consumption rate (mtOCR) and ATP coupling of mature osteoclasts cultured under normoxia with 10 mM lactate or untreated. Mean ± SE, $N = 3$, $n = 7$. $^{*}p < 0.05$ and $^{**}p < 0.01$ *vs* untreated. (c) Emission spectra of JC-1 to measure the mitochondrial potential of osteoclasts cultured with lactate or untreated. JC-1 monomers emit green fluorescence (540 nm); aggregates emit orange-red fluorescence (590 nm). Upper panel, graph showing the ratio of 590/540 emission. Lower panel, representative images and the spectra from the mitochondria of a single cell in the respective conditions. Scale bar, 30 μm. (d) Quantification of the JC1 signal by spectral confocal microscopy of the JC-1 fluorescence intensity of osteoclasts cultured with lactate or untreated. Mean ± SE, $n = 42$ cells from 3 independent experiments. $^{***}p < 0.001$ *vs* untreated. (e) Glycolytic efficiency (glucose consumption/lactate production ratio) of osteoclasts cultured with 10 mM lactate or untreated. Mean ± SE, $N = 3$, $n = 5$. $^{****}p < 0.0001$ *vs* untreated.

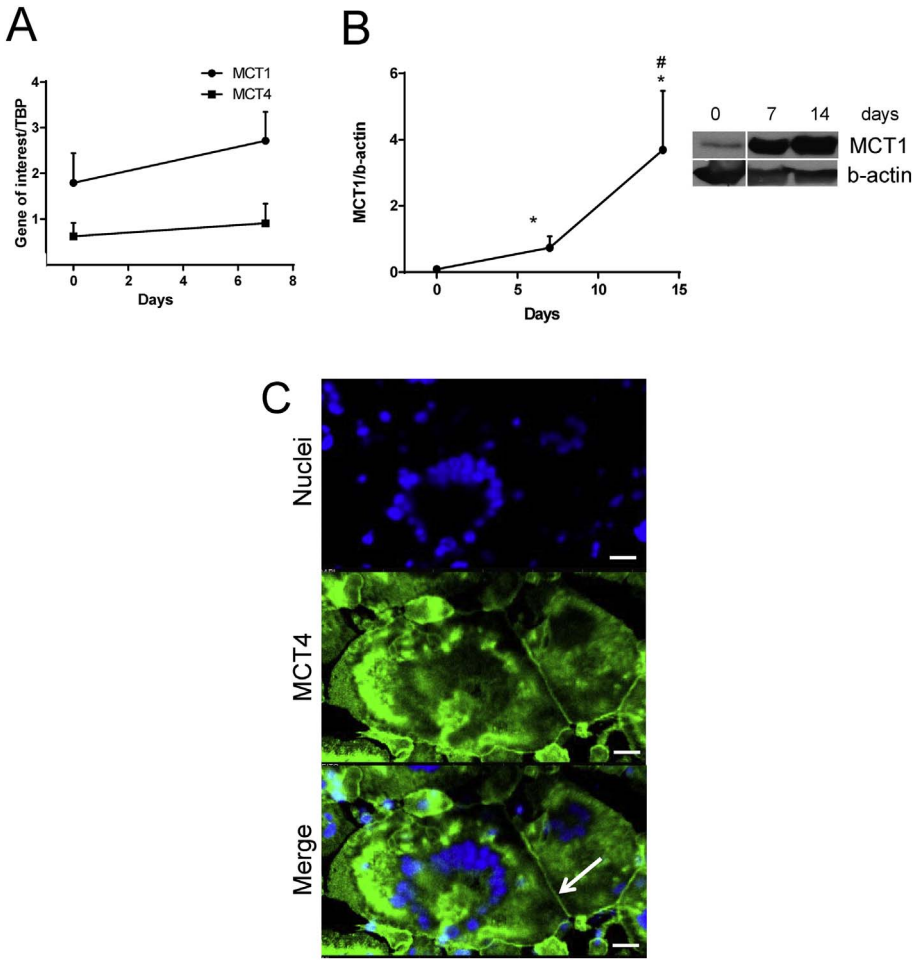

Fig. 4. MCT1 expression increases along the osteoclast differentiation process. (a) MCT1 and MCT4 mRNA expression of osteoclast precursors (0 day of differentiation) and mature osteoclasts (7 days of differentiation). Mean ± SE, $N = 3$. (b) Western blot analysis of MCT1 expression in osteoclast precursors (0 day), mature osteoclasts (7 days) and fully differentiated osteoclasts (14 days). Right panel, representative image. Mean ± SE, $N = 3$. *$p < 0.05$ *vs* 0 day, #$p < 0.05$ *vs.* 7 days of differentiation. (c) Representative image of confocal analysis of immunofluorescence staining of MCT4 (green) in cell cultures of mature osteoclasts. The osteoclast phenotype was confirmed by multinuclearity (blue). MCT4 localized at the plasma membrane (white arrow). Scale bar, 20 μm.

expression was significantly higher in osteoclasts than in precursor cells (Fig. 4B, $p < 0.05$). MCT4 localized at the plasma membrane of mature multinucleated osteoclasts (Fig. 4C). These results collectively establish that the expression of MCT1 increases during osteoclastogenesis, and that MCT4 localized at the plasma membrane of fully differentiated osteoclasts.

3.4. Targeting MCT1 impairs lactate-promoted osteoclast activity

We next aimed to study the functional consequences of lactate uptake by osteoclasts, and focused on the bone resorption activity that is commonly associated with BM. Osteoclast precursors were seeded on a layer of collagenous matrix and exposed to 10 mM of sodium lactate. Lactate-based treatment significantly increased Type I collagen degradation (Fig. 5A, $p = 0.0003$) confirming our hypothesis: glycolytic breast cancer cells in the bone microenvironment release lactate that is then uptaken and oxidized by bone resorbing osteoclasts. Notably, we have recently demonstrated that bone resorption activity of osteoclasts is indirectly dependent by oxidative metabolism since this metabolic pathway is fundamental to maintain osteoclast survival [29]. Furthermore, it may be hypothesized that an increase of oxidative metabolism at the presence of simultaneously active glycolysis directly fuels the highly energy consuming biological process of bone resorption. According to this hypothesis, we tested whether 7ACC2, an inhibitor of lactate uptake that does not inhibit lactate export [30], may decrease osteoclast differentiation and activity. For this aim, we used conditioned medium (CM) obtained from MDA-MB-231 cells, containing about 10 mM lactate (Fig. 1E), or pro-osteoclastogenic medium supplemented with sodium lactate at the same concentration, and found that MDA-MB-231 supernatant induced osteoclastogenesis (Fig. 5B). Inhibition of lactate uptake with 7ACC2 did not affect osteoclast formation in CM-treated or lactate-treated conditions (Fig. 5B–C), which was confirmed by showing a small and not significant trend of decreased expression of the osteoclast-related marker cathepsin K (CTSK) and no change in the mRNA expression of matrix metalloproteinase 9 (MMP9) (Fig. 5D). Thus, CM promoted osteoclastogenesis in a lactate-independent manner. Conversely, Type I collagen degradation was inhibited by 7ACC2, that significantly decreased both tumor-promoted and lactate-promoted Type I collagen resorption (Fig. 5E, $p = 0.0175$ and $p = 0.0006$, respectively). Taken together, our results highlight that lactate released by MDA-MB-231 cells and uptaken by osteoclasts facilitates the bone resorption activity without stimulating osteoclastogenesis, and that MCT1 targeting impairs bone resorption in osteolytic BM (Fig. 5F).

4. Discussion

Several lines of evidence suggest that the acquisition of the metastatic phenotype is associated with a series of metabolic adaptations of cancer cells. For example, an altered metabolic flux increases the release of lactate into the tumor microenvironment, which is associated with a higher metastatic potential in cancer [24]. However, despite the efforts spent exploring the effect of lactate on tumor progression, its exact role in cancer, and especially in BM, remains elusive. Using two human breast carcinoma models with different levels of aggressiveness, we confirm that the most aggressive cell line, that is capable to develop BM *in vivo*, as previously demonstrated by others [38,39], display a Warburg phenotype characterized by an increased NADH/NAD^+ ratio,

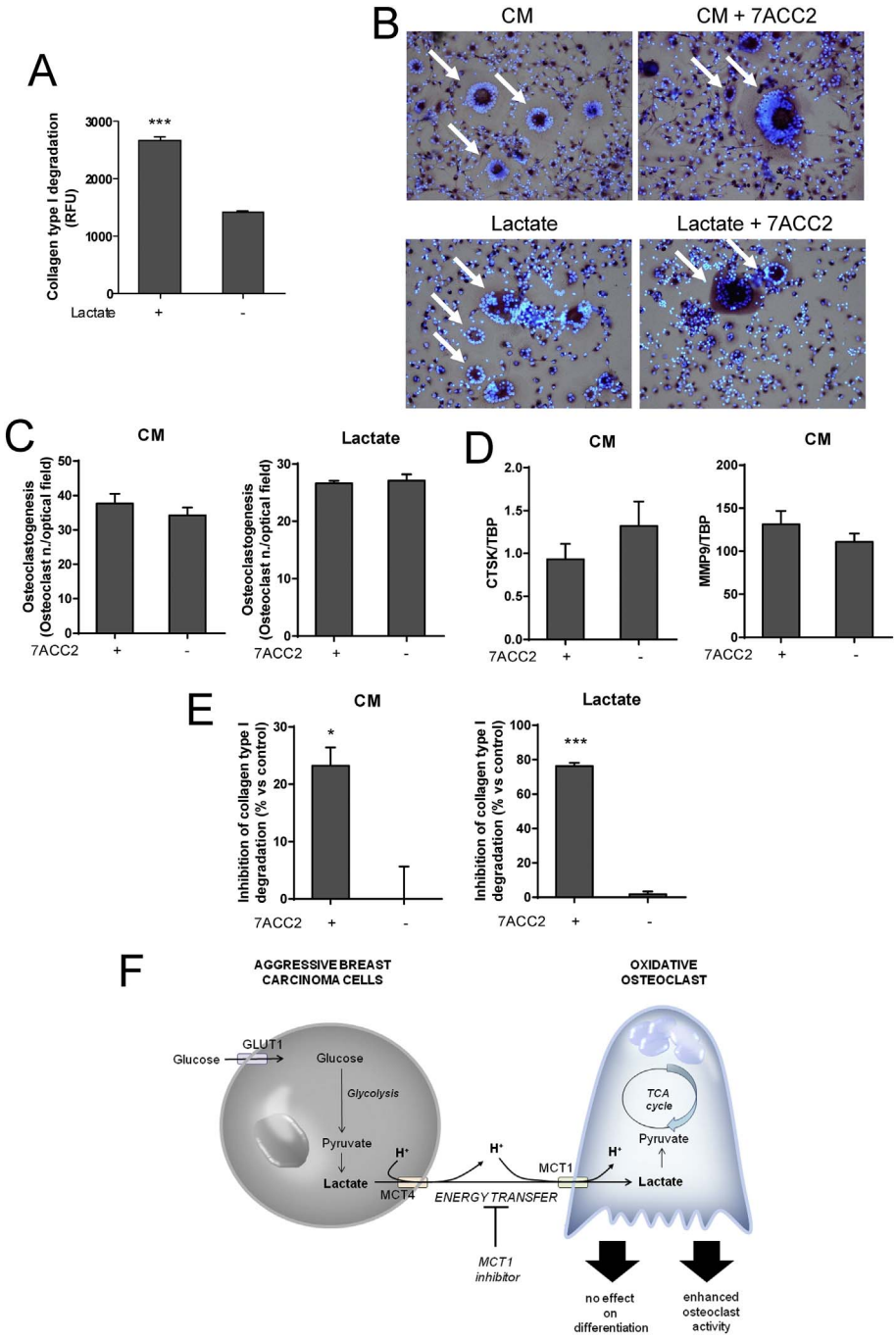

Fig. 5. Lactate uptake inhibitor 7ACC2 impairs lactate-induced bone resorption by osteoclasts without affecting osteoclastogenesis. Different conditions were used to study differentiated osteoclasts, including incubation with MDA-MB-231 supernatant (conditioned media, CM) or with pro-osteoclastogenic medium supplemented with lactate with or without 7ACC2. (a) Type I collagen degradation by osteoclasts cultured with 10 mM of sodium lactate or untreated. Mean ± SE, $N = 2$, $n = 4$, $^{***}p < 0.001$ *vs* untreated. (b) Representative images of TRACP and nuclear staining of osteoclast cultures. White arrows show multinucleated $TRACP^{+}$ cells. (c) Number of obtained osteoclasts, mean ± SE, $N = 3$. (d) Cathepsin K (CTSK) and metalloproteinase 9 (MMP9) mRNA expression in mature osteoclasts. Mean ± SE, $N = 2$, $n = 2$. (e) Type I collagen degradation activity. Mean ± SE, $N = 2$, $n = 4$. $^{*}p < 0.05$ and $^{***}p < 0.001$ *vs* untreated. (f) Schematic representation of the coupling between breast carcinoma cells and mature osteoclasts in the microenvironment of a bone metastasis. Lactate released by glycolytic cancer cells *via* MCT4 is taken up by oxidative osteoclasts *via* MCT1, where it fuels the TCA cycle. Lactate influx inhibitor 7ACC2 inhibits this process.

GLUT1 expression, glycolytic rate, and, as a result, increased release of lactate in the extracellular microenvironment. On the contrary, the metabolism of the less-aggressive breast carcinoma cells is mainly based on oxidative phosphorylation.

According to previous reports, extracellular lactate can be used as an energy source when it is imported by oxidative cells in a process facilitated by passive lactate-proton symporters of the MCT family [40]. Among different isoforms, MCT1 is the most widely expressed and has been detected at the plasma membrane of skeletal muscle fibers, hepatocytes, and cardiac cells, where it mediates lactate uptake [41]. Conversely, MCT4 facilitates the release of lactate into the extracellular environment, is detected at the plasma membrane of glycolytic cells, including white muscle fibers, and its expression is induced by hypoxia [42]. Our data confirm that in MDA-MB-231 cells MCT1 is poorly expressed, possibly because the CpG island in the 5′ upstream region of the MCT1 gene is methylated [43], whereas MCT4 expression is quite high, both under hypoxic and normoxic conditions. These results confirm that MDA-MB-231 cells own a Warburg phenotype. Notably, we also showed MCT4 expression in cancer cells metastatic to the bone. Recent reports have indicated that lactate acts as an energy-transfer molecule in the tumor microenvironment by fueling several energy-consuming processes in cancer-associated stromal cells [27] and by promoting a metabolic symbiosis between glycolytic and oxidative cells [28]. In particular, fibroblasts and mesenchymal stromal cells can use lactate released by cancer cells as an energy source [44], whereas endothelial cells use lactate both as a signaling molecule and as a metabolic intermediate that stimulates neo-angiogenesis [26]. Likewise, our study demonstrates that lactate produced by glycolytic cancer cells is a metabolic fuel also for osteoclasts. We have previously reported that differentiated osteoclasts are in a high energy state and that the energy

required for osteoclastogenesis is mainly derived from mitochondrial metabolism. In addition, in active osteoclasts during bone resorption, mitochondrial metabolism is also associated with glycolysis, as high glucose concentration (20 mM) fuels the resorption activity of osteoclasts [29]. However, when metastatic carcinoma cells colonize bone, they are exposed to a hypoxic environment [45] that further prompts them to consume large amounts of glucose that fuel glycolytic metabolism and enhance lactate production. Thus, it can be speculated that, due to the mentioned tumor consumption of glucose and high lactate production, the other cells in the BM environment, including osteoclasts, can only rely on low levels of glucose and high levels of extracellular lactate. Accordingly, to recapitulate the BM microenvironment *in vitro*, we developed a medium with reduced glucose (2 mM) [46], balanced with 10 mM of lactate, a concentration that is frequently detected in breast carcinoma [37], and that also corresponds to the concentration observed in the supernatant of aggressive breast carcinoma cells MDA-MB-231.

As a confirmation of the exchange of lactate between cancer cells and osteoclasts, we found that osteoclasts uptake exogenous lactate that promoted a higher bioenergetic state by fueling mitochondrial metabolism, as demonstrated by enhanced OCR, enhanced ATP coupling, enhanced mitochondrial membrane potential, and reduced glycolytic efficiency. As a consequence of lactate uptake, the differentiation process was not affected, whereas Type I collagen degradation activity was significantly enhanced. If these results are translated to the *in vivo* setting, it is interesting to note that the effect of enhanced bone resorption induced by lactate uptake mediated by MCT1 in osteoclasts might also derive from an enhanced intracellular acidification as a result of hydrogen ion symport with lactate by MCT1. Indeed, the acidification of lysosomes is a crucial step for bone resorption activity [47]. We also provide evidence that osteoclasts may uptake the extracellular lactate *via* MCT1 since, as previously shown [48], the expression levels of MCT1 are increased whereas MCT4 expression is not changed.

Thus, as a subsequent step, we tested and validated the role of MCT1 as a major player in lactate metabolic coupling between cancer cells and osteoclasts and as a possible therapeutic target for the treatment of patients with BM. We used the MCT1 inhibitor 7ACC2 (IC_{50} = 11 nM on ^{14}C-lactate flux inhibition) that was previously demonstrated to delay the growth of human cervix SiHa, colorectal HCT116 and orthotopic MCF7 breast cancer *in vivo* [30]. MCT targeting has been already considered for clinical trial in cancer. AZD39965, a dual MCT1 and MCT2 inhibitor, is being evaluated as anticancer agent in a Phase I clinical trial for patients with advanced prostate cancer, gastric cancer, or diffuse large B cell lymphoma (ClinicalTrials.gov NCT01791595). *In vivo*, AZD39965 enhanced the sensitivity of solid tumors to radiotherapy, suggesting that combining anti-MCT therapies with other treatments is a promising therapeutic approach [49]. In our study, treatment with 7ACC2 did not affect osteoclast formation in the presence of lactate-containing conditioned medium of breast carcinoma cells or lactate-enriched medium. Similarly, the mRNA expression of osteoclast-markers cathepsin K [50] and MMP9 [51] was unchanged after treatment with a MCT1 inhibitor. In contrast, the pharmacological inhibition of lactate uptake by 7ACC2 impaired the bone resorption activity of osteoclasts, either stimulated by tumor-derived lactate or by lactate present in the CM of human breast cancer cells.

The new concept of osteolytic BM here envisioned goes beyond the classical “vicious cycle model,” according to which osteoclast stimulation is triggered only by a paracrine secretion of cytokines and protein factors from cancer cells. Our concept identifies key players of tumor-stroma metabolic interplay, such as MCT1 that deserves further investigation to be considered as a possible novel therapeutic target for this condition. Indeed, in our model, oxidative osteoclasts recycle lactate that is produced by glycolytic cancer cells *via* MCT1, ultimately supporting cancer-associated osteolytic lesions and fostering a more aggressive tumor phenotype.

Funding sources

This work was supported by the Italian Association for Cancer Research (AIRC MFAG to SA n. 14191), financial support for Scientific Research “5 per 1000 2014” to NB, a Starting Grant from the European Research Council (ERC 243188 TUMETABO) to PS, Attraction Pole (IAP) grant #UP7-03 from the Belgian Science Policy Office (Belspo) to PS, an Action de Recherche Concertée from the Communauté Française de Belgique (ARC 14/19-058) to PS and the Belgian Fonds National de la Recherche Scientifique (F.R.S.-FNRS short stay grant 2014/V 6/5/006-LID-6394 to SL). Funding sources had no rules in study design, conducting the research, data analysis, preparation of the article, or decision to submit the article for publication.

Author contributions

Author contributions: study conception (SA), work design (SL, PS, SA, SR, NB, RG, PEP), data collection (SL, GDP, SR, PEP, MS), analysis and interpretation of data (SL, PS, SA, RG, GDP, PEP, SR, MS), drafting of manuscript (SL, NB, SA), critical revision (PS, NB, GDP, RG, MS, SR, PEP).

Transparency document

The Transparency document associated with this article can be found, in online version.

Acknowledgements

The authors thank at Rizzoli Orthopaedic Institute Marta Columbaro for frozen tissue sectioning, at the Université catholique de Louvain (UCL) Prof. Olivier Feron for kindly providing 7ACC2, Jhudit Pérez-Escuredo for the experimental assistance in ^{14}C-sodium lactate uptake assay analysis.

References

[1] K.N. Weilbaecher, T.A. Guise, L.K. McCauley, Cancer to bone: a fatal attraction, Nat. Rev. Cancer 11 (2011) 411–425, http://dx.doi.org/10.1038/nrc3055.
[2] T. Wada, T. Nakashima, N. Hiroshi, J.M. Penninger, RANKL-RANK signaling in osteoclastogenesis and bone disease, Trends Mol. Med. 12 (2006) 17–25, http://dx.doi.org/10.1016/j.molmed.2005.11.007.
[3] W.J. Boyle, W.S. Simonet, D.L. Lacey, Osteoclast differentiation and activation, Nature 423 (2003) 337–342, http://dx.doi.org/10.1038/nature01658.
[4] G.R. Mundy, T.A. Guise, Hypercalcemia of malignancy, Am. J. Med. 103 (1997) 134–145.
[5] R.E. Coleman, Clinical features of metastatic bone disease and risk of skeletal morbidity, Clin. Cancer Res. 12 (2006) 6243s–6249s, http://dx.doi.org/10.1158/1078-0432.CCR-06-0931.
[6] A.F. Chambers, A.C. Groom, I.C. MacDonald, Dissemination and growth of cancer cells in metastatic sites, Nat. Rev. Cancer 2 (2002) 563–572, http://dx.doi.org/10.1038/nrc865.
[7] T. Yoneda, T. Hiraga, Crosstalk between cancer cells and bone microenvironment in bone metastasis, Biochem. Biophys. Res. Commun. 328 (2005) 679–687, http://dx.doi.org/10.1016/j.bbrc.2004.11.070.
[8] T. Hiraga, S. Kizaka-Kondoh, K. Hirota, M. Hiraoka, T. Yoneda, Hypoxia and hypoxia-inducible factor-1 expression enhance osteolytic bone metastases of breast cancer, Cancer Res. 67 (2007) 4157–4163, http://dx.doi.org/10.1158/0008-5472.CAN-06-2355.
[9] T.A. Guise, The vicious cycle of bone metastases, J. Musculoskelet. Neuronal Interact. 2 (2002) 570–572.
[10] R.R. Langley, I.J. Fidler, The seed and soil hypothesis revisited–the role of tumor-stroma interactions in metastasis to different organs, Int. J. Cancer 128 (2011) 2527–2535, http://dx.doi.org/10.1002/ijc.26031.
[11] G.J. Powell, J. Southby, J.A. Danks, R.G. Stillwell, J.A. Hayman, M.A. Henderson, R.C. Bennett, T.J. Martin, Localization of parathyroid hormone-related protein in breast cancer metastases: increased incidence in bone compared with other sites, Cancer Res. 51 (1991) 3059–3061.
[12] K. Kobayashi, N. Takahashi, E. Jimi, N. Udagawa, M. Takami, S. Kotake, N. Nakagawa, M. Kinosaki, K. Yamaguchi, N. Shima, H. Yasuda, T. Morinaga, K. Higashio, T.J. Martin, T. Suda, Tumor necrosis factor alpha stimulates osteoclast differentiation by a mechanism independent of the ODF/RANKL-RANK interaction, J. Exp. Med. 191 (2000) 275–286.
[13] O. Kudo, A. Sabokbar, A. Pocock, I. Itonaga, Y. Fujikawa, N.A. Athanasou,

Interleukin-6 and interleukin-11 support human osteoclast formation by a RANKL-independent mechanism, Bone 32 (2003) 1–7.
[14] S. Avnet, M. Salerno, G. Quacquaruccio, D. Granchi, A. Giunti, N. Baldini, IGF2 derived from SH-SY5Y neuroblastoma cells induces the osteoclastogenesis of human monocytic precursors, Exp. Cell Res. 317 (2011) 2147–2158, http://dx.doi.org/10.1016/j.yexcr.2011.05.030.
[15] I. Itonaga, A. Sabokbar, S.G. Sun, O. Kudo, L. Danks, D. Ferguson, Y. Fujikawa, N.A. Athanasou, Transforming growth factor-beta induces osteoclast formation in the absence of RANKL, Bone 34 (2004) 57–64.
[16] D. Granchi, I. Amato, L. Battistelli, S. Avnet, S. Capaccioli, L. Papucci, M. Donnini, A. Pellacani, M.L. Brandi, A. Giunti, N. Baldini, In vitro blockade of receptor activator of nuclear factor-kappaB ligand prevents osteoclastogenesis induced by neuroblastoma cells, Int. J. Cancer 111 (2004) 829–838, http://dx.doi.org/10.1002/ijc.20308.
[17] G.G. Steger, R. Bartsch, Denosumab for the treatment of bone metastases in breast cancer: evidence and opinion, Ther. Adv. Med. Oncol. 3 (2011) 233–243, http://dx.doi.org/10.1177/1758834011412656.
[18] A.J. Levine, A.M. Puzio-Kuter, The control of the metabolic switch in cancers by oncogenes and tumor suppressor genes, Science 330 (2010) 1340–1344, http://dx.doi.org/10.1126/science.1193494.
[19] V.L. Payen, P.E. Porporato, B. Baselet, P. Sonveaux, Metabolic changes associated with tumor metastasis, part 1: tumor pH, glycolysis and the pentose phosphate pathway, Cell. Mol. Life Sci. 73 (2016) 1333–1348, http://dx.doi.org/10.1007/s00018-015-2098-5.
[20] M.W. Dewhirst, Mechanisms underlying hypoxia development in tumors, Adv. Exp. Med. Biol. 510 (2003) 51–56.
[21] O. Warburg, On the origin of cancer cells, Science 123 (1956) 309–314.
[22] R.A. Gatenby, R.J. Gillies, Why do cancers have high aerobic glycolysis? Nat. Rev. Cancer 4 (2004) 891–899, http://dx.doi.org/10.1038/nrc1478.
[23] S. Dhup, R.K. Dadhich, P.E. Porporato, P. Sonveaux, Multiple biological activities of lactic acid in cancer: influences on tumor growth, angiogenesis and metastasis, Curr. Pharm. Des. 18 (2012) 1319–1330.
[24] S. Walenta, M. Wetterling, M. Lehrke, G. Schwickert, K. Sundfor, E.K. Rofstad, W. Mueller-Klieser, High lactate levels predict likelihood of metastases, tumor recurrence, and restricted patient survival in human cervical cancers, Cancer Res. 60 (2000) 916–921.
[25] F. Vegran, R. Boidot, C. Michiels, P. Sonveaux, O. Feron, Lactate influx through the endothelial cell monocarboxylate transporter MCT1 supports an NF-kappaB/IL-8 pathway that drives tumor angiogenesis, Cancer Res. 71 (2011) 2550–2560, http://dx.doi.org/10.1158/0008-5472.CAN-10-2828.
[26] P. Sonveaux, T. Copetti, C.J. De Saedeleer, F. Vegran, J. Verrax, K.M. Kennedy, E.J. Moon, S. Dhup, P. Danhier, F. Frerart, B. Gallez, A. Ribeiro, C. Michiels, M.W. Dewhirst, O. Feron, Targeting the lactate transporter MCT1 in endothelial cells inhibits lactate-induced HIF-1 activation and tumor angiogenesis, PLoS One 7 (2012) e33418, , http://dx.doi.org/10.1371/journal.pone.0033418.
[27] G. Bonuccelli, S. Avnet, G. Grisendi, M. Salerno, D. Granchi, M. Dominici, K. Kusuzaki, N. Baldini, Role of mesenchymal stem cells in osteosarcoma and metabolic reprogramming of tumor cells, Oncotarget 5 (2014) 7575–7588, http://dx.doi.org/10.18632/oncotarget.2243.
[28] P. Sonveaux, F. Vegran, T. Schroeder, M.C. Wergin, J. Verrax, Z.N. Rabbani, C.J. De Saedeleer, K.M. Kennedy, C. Diepart, B.F. Jordan, M.J. Kelley, B. Gallez, M.L. Wahl, O. Feron, M.W. Dewhirst, Targeting lactate-fueled respiration selectively kills hypoxic tumor cells in mice, J. Clin. Invest. 118 (2008) 3930–3942, http://dx.doi.org/10.1172/JCI36843.
[29] S. Lemma, M. Sboarina, P.E. Porporato, N. Zini, P. Sonveaux, G. Di Pompo, N. Baldini, S. Avnet, Energy metabolism in osteoclast formation and activity, Int. J. Biochem. Cell Biol. 79 (2016) 168–180, http://dx.doi.org/10.1016/j.biocel.2016.08.034.
[30] N. Draoui, O. Schicke, E. Seront, C. Bouzin, P. Sonveaux, O. Riant, O. Feron, Antitumor activity of 7-aminocarboxycoumarin derivatives, a new class of potent inhibitors of lactate influx but not efflux, Mol. Cancer Ther. 13 (2014) 1410–1418, http://dx.doi.org/10.1158/1535-7163.MCT-13-0653.
[31] D. Cappellen, N.H. Luong-Nguyen, S. Bongiovanni, O. Grenet, C. Wanke, M. Susa, Transcriptional program of mouse osteoclast differentiation governed by the macrophage colony-stimulating factor and the ligand for the receptor activator of NFkappa B, J. Biol. Chem. 277 (2002) 21971–21982, http://dx.doi.org/10.1074/jbc.M200434200.
[32] S. Lemma, S. Avnet, M. Salerno, T. Chano, N. Baldini, Identification and validation of housekeeping genes for gene expression analysis of cancer stem cells, PLoS One 11 (2016) e0149481, , http://dx.doi.org/10.1371/journal.pone.0149481.
[33] J. Doyen, C. Trastour, F. Ettore, I. Peyrottes, N. Toussant, J. Gal, K. Ilc, D. Roux, S.K. Parks, J.M. Ferrero, J. Pouyssegur, Expression of the hypoxia-inducible monocarboxylate transporter MCT4 is increased in triple negative breast cancer and correlates independently with clinical outcome, Biochem. Biophys. Res. Commun. 451 (2014) 54–61, http://dx.doi.org/10.1016/j.bbrc.2014.07.050.
[34] D.M. Stover, I. Carey, R.J. Garzon, Z.E. Zehner, A negative regulatory factor is missing in a human metastatic breast cancer cell line, Cancer Res. 54 (1994) 3092–3095.
[35] K.S. Dimmer, B. Friedrich, F. Lang, J.W. Deitmer, S. Broer, The low-affinity monocarboxylate transporter MCT4 is adapted to the export of lactate in highly glycolytic cells, Biochem. J. 350 (Pt 1) (2000) 219–227.
[36] J. Perez-Escuredo, V.F. Van Hee, M. Sboarina, J. Falces, V.L. Payen, L. Pellerin, P. Sonveaux, Monocarboxylate transporters in the brain and in cancer, Biochim. Biophys. Acta 1863 (2016) 2481–2497, http://dx.doi.org/10.1016/j.bbamcr.2016.03.013.
[37] S. Walenta, S. Snyder, Z.A. Haroon, R.D. Braun, K. Amin, D. Brizel, W. Mueller-Klieser, B. Chance, M.W. Dewhirst, Tissue gradients of energy metabolites mirror oxygen tension gradients in a rat mammary carcinoma model, Int. J. Radiat. Oncol. Biol. Phys. 51 (2001) 840–848.
[38] I.F. Robey, R.M. Stephen, K.S. Brown, B.K. Baggett, R.A. Gatenby, R.J. Gillies, Regulation of the Warburg effect in early-passage breast cancer cells, Neoplasia 10 (2008) 745–756.
[39] I.F. Robey, A.D. Lien, S.J. Welsh, B.K. Baggett, R.J. Gillies, Hypoxia-inducible factor-1alpha and the glycolytic phenotype in tumors, Neoplasia 7 (2005) 324–330.
[40] A.P. Halestrap, N.T. Price, The proton-linked monocarboxylate transporter (MCT) family: structure, function and regulation, Biochem. J. 343 (Pt 2) (1999) 281–299.
[41] S.K. Baker, K.J. McCullagh, A. Bonen, Training intensity-dependent and tissue-specific increases in lactate uptake and MCT-1 in heart and muscle, J. Appl. Physiol. 84 (1998) 987–994.
[42] M.S. Ullah, A.J. Davies, A.P. Halestrap, The plasma membrane lactate transporter MCT4, but not MCT1, is up-regulated by hypoxia through a HIF-1alpha-dependent mechanism, J. Biol. Chem. 281 (2006) 9030–9037, http://dx.doi.org/10.1074/jbc.M511397200.
[43] K. Asada, K. Miyamoto, T. Fukutomi, H. Tsuda, Y. Yagi, K. Wakazono, S. Oishi, H. Fukui, T. Sugimura, T. Ushijima, Reduced expression of GNA11 and silencing of MCT1 in human breast cancers, Oncology 64 (2003) 380–388 (70297).
[44] Y.I. Rattigan, B.B. Patel, E. Ackerstaff, G. Sukenick, J.A. Koutcher, J.W. Glod, D. Banerjee, Lactate is a mediator of metabolic cooperation between stromal carcinoma associated fibroblasts and glycolytic tumor cells in the tumor microenvironment, Exp. Cell Res. 318 (2012) 326–335, http://dx.doi.org/10.1016/j.yexcr.2011.11.014.
[45] J.A. Spencer, F. Ferraro, E. Roussakis, A. Klein, J. Wu, J.M. Runnels, W. Zaher, L.J. Mortensen, C. Alt, R. Turcotte, R. Yusuf, D. Cote, S.A. Vinogradov, D.T. Scadden, C.P. Lin, Direct measurement of local oxygen concentration in the bone marrow of live animals, Nature 508 (2014) 269–273, http://dx.doi.org/10.1038/nature13034.
[46] J.P. Williams, H.C. Blair, J.M. McDonald, M.A. McKenna, S.E. Jordan, J. Williford, R.W. Hardy, Regulation of osteoclastic bone resorption by glucose, Biochem. Biophys. Res. Commun. 235 (1997) 646–651, http://dx.doi.org/10.1006/bbrc.1997.6795.
[47] J. Lacombe, G. Karsenty, M. Ferron, Regulation of lysosome biogenesis and functions in osteoclasts, Cell Cycle 12 (2013) 2744–2752, http://dx.doi.org/10.4161/cc.25825.
[48] H. Ahn, K. Lee, J.M. Kim, S.H. Kwon, S.H. Lee, S.Y. Lee, D. Jeong, Accelerated lactate dehydrogenase activity potentiates osteoclastogenesis via NFATc1 signaling, PLoS One 11 (2016) e0153886, , http://dx.doi.org/10.1371/journal.pone.0153886.
[49] B.M. Bola, A.L. Chadwick, F. Michopoulos, K.G. Blount, B.A. Telfer, K.J. Williams, P.D. Smith, S.E. Critchlow, I.J. Stratford, Inhibition of monocarboxylate transporter-1 (MCT1) by AZD3965 enhances radiosensitivity by reducing lactate transport, Mol. Cancer Ther. 13 (2014) 2805–2816, http://dx.doi.org/10.1158/1535-7163.MCT-13-1091.
[50] S. Avnet, A. Lamolinara, N. Zini, L. Solimando, G. Quacquaruccio, D. Granchi, N.M. Maraldi, A. Giunti, N. Baldini, Effects of antisense mediated inhibition of cathepsin K on human osteoclasts obtained from peripheral blood, J. Orthop. Res. 24 (2006) 1699–1708, http://dx.doi.org/10.1002/jor.20209.
[51] K. Sundaram, R. Nishimura, J. Senn, R.F. Youssef, S.D. London, S.V. Reddy, RANK ligand signaling modulates the matrix metalloproteinase-9 gene expression during osteoclast differentiation, Exp. Cell Res. 313 (2007) 168–178, http://dx.doi.org/10.1016/j.yexcr.2006.10.001.